0026-895X/01/5905-1077–1085$3.00
MOLECULAR PHARMACOLOGY
Copyright © 2001 The American Society for Pharmacology and Experimental Therapeutics
Mol Pharmacol 59:1077–1085, 2001

Vol. 59, No. 5
621/899059
Printed in U.S.A.

Charged Amino Acids in the Transmembrane Domains Are Involved in the Determination of the Substrate Specificity of Rat Mrp2

KOUSEI ITO,[1] HIROSHI SUZUKI, and YUICHI SUGIYAMA

Graduate School of Pharmaceutical Sciences, The University of Tokyo, Tokyo, Japan

Received October 5, 2000; accepted January 19, 2001

This paper is available online at http://molpharm.aspetjournals.org

ABSTRACT

Multidrug resistance-associated protein 2 (MRP2) transports glutathione conjugates, glucuronide conjugates, and sulfated conjugates of bile acids. In the present study, we examined the role of charged amino acids in the transmembrane domains of rat Mrp2, conserved among MRP families, using the isolated membrane vesicles from Sf9 cells infected with the recombinant baculoviruses. By normalizing the transport activity for compounds by that for estradiol 17β-D-glucuronide ($E_2$17βG), it was indicated that the site-directed mutagenesis from Lys to Met at 325 (K325M) and from Arg to Leu at 586 (R586L) results in a marked reduction in the transport for glutathione conjugates [2,4-dinitrophenyl-*S*-glutathione (DNP-SG) and leukotriene (LT) C_4] without affecting that for 6-hydroxy-5,7-dimethyl-2-methylamino-4-(3-pyridymethyl) benzothiazole glucuronide and taurolithocholate sulfate. In contrast to the reduced affinity for DNP-SG, the affinity for $E_2$17βG was increased severalfold in these mutant Mrp2s, suggesting the amino acids at 325 and 586 play an important role in distinguishing between glutathione and glucuronide conjugates. The comparable affinity for LTD_4, LTE_4, and LTF_4 in these mutant Mrp2s with that in wild-type Mrp2 indicates that recognition of LTC_4 metabolites by Mrp2 is different from that of LTC_4. The transport activity for glutathione conjugate was retained on R586K, whereas no such complementary cationic amino acid effect was observed in K325R. In addition, R1206M and E1208Q exhibited the loss of transport activity for the tested compounds. The results of the present study demonstrate that the charged amino acids in the transmembrane domain of rat Mrp2 may play an important role in the recognition and/or transport of its substrates.

Canalicular multispecific organic anion transporter/multidrug resistance-associated protein 2 (cMOAT/MRP2) plays an important role in the biliary excretion of anionic compounds. In patients suffering from Dubin-Johnson syndrome, a defect in the expression of this protein has been demonstrated (Kartenbeck et al., 1996; Paulusma et al., 1997; Toh et al., 1999; Tsujii et al., 1999). The substrate specificity of Mrp2 has been determined in great detail by comparing transport across the bile canalicular membrane between normal and Mrp2-deficient rats (Keppler and König, 1997; Suzuki and Sugiyama, 1998). Mrp2 substrates include glutathione conjugates [e.g., 2, 4-dinitrophenyl-*S*-glutathione (DNP-SG) and leukotriene (LT) C_4], glucuronide conjugates [e.g., estradiol 17-β-D-glucuronide ($E_2$17βG)], sulfate conjugates of certain bile salts [e.g., taurolithocholate-3-sulfate (TLC-S)], and nonconjugated organic anions (e.g., methotrexate) (Keppler and König, 1997; Suzuki and Sugiyama, 1998). As a homolog of MRP1, the cDNA for Mrp2/MRP2 has been cloned (Büchler et al., 1996; Paulusma et al., 1996; Taniguchi et al., 1996; Ito et al., 1997) and a functional analysis of the cloned cDNA product has been performed (Madon et al., 1997; Evers et al., 1998; Ito et al., 1998; van Aubel et al., 1998; Cui et al., 1999). The substrate specificity of Mrp2/MRP2 is very similar to that of MRP1 (Gao et al., 1996; Keppler and König, 1997; Cole and Deeley, 1998; Suzuki and Sugiyama, 1998; Cui et al., 1999).

More recently, rat and human Mrp3/MRP3 have been cloned as a homolog of MRP1 and 2 (Hirohashi et al., 1998;

This work was supported by a Grant-in-Aid for Scientific Research on Priority Areas "ABC proteins" 10044243 from the Ministry of Education, Science, and Culture of Japan.

The present study has been presented in part at the 91th Annual Meeting of American Association for Cancer Research, San Francisco, California, 2000 April 1–5. It appeared as an abstract in the published proceedings of this meeting [Proceedings of the American Association for Cancer Research (2000) **41:**673].

[1] Current address: Faculty of Pharmaceutical Sciences, Chiba University, Yayoi-cho 1-33, Inage-ku, Chiba, 263-8522, Japan.

ABBREVIATIONS: cMOAT/MRP, canalicular multispecific organic anion transporter/multidrug resistance-associated protein; DNP-SG, 2,4-dinitrophenyl-*S*-glutathione; LT, leukotriene; $E_2$17βG, estradiol 17-β-D-glucuronide; E3040, 6-hydroxy-5,7-dimethyl-2-methylamino-4-(3-pyridymethyl) benzothiazole; TLC-S, taurolithocholate-3-sulfate; TM, transmembrane domains; MSD, membrane-spanning domain regions; NBD, nucleotide-binding domain; CFTR, cystic fibrosis conductance regulator; GFP, green fluorescent protein; CMV, canalicular membrane vesicle; ANOVA, analysis of variance.

Kiuchi et al., 1998; Uchiumi et al., 1998; Kool et al., 1999). Considering the fact that rat and human MRP3s are highly expressed on the basolateral membrane of rat and human liver under cholestatic/hyperbilirubinemic conditions (König et al., 1999; Kool et al., 1999), it is possible that Mrp3/MRP3 may compensate for the impaired function of cMOAT/MRP2 in the liver. Hirohashi et al. (1999) were the first to demonstrate that the substrate specificity of rat Mrp3 is markedly different from MRP1 and cMOAT/MRP2 in that although glucuronide conjugates, such as $E_2$17βG and E3040-glucuronide, or nonconjugated organic anions, such as methotrexate, are good substrates, glutathione conjugates, such as DNP-SG and LTC_4, are poor substrates for Mrp3. A hydropathy plot analysis suggests that the structures of MRP1–3 are very similar.

The substrate recognition/transport by MRP1 has been studied in relation to its structure. MRP1 consists of 17 transmembrane domains (TMs) organized in three membrane-spanning domain regions [MSD1 (TM1–5), MSD2 (TM6–11), and MSD3 (TM12–17)] (Deeley and Cole, 1997). The function of MSD1 followed by a linker region, both of which are not present in MDR-type transporters, was studied using a series of 5′-truncated MRP1 molecules expressed in insect cells (Bakos et al., 1998; Gao et al., 1998). They found that the linker region between MSD1 and 2, but not the MSD1 domain itself, is necessary for transporting LTC_4. Moreover, a chimeric study of human MRP1 and mouse mrp1 expressed in human embryonic kidney 293 cells suggested that anthracycline resistance and the ability to transport $E_2$17βG is conferred by the COOH-terminal third of the protein (Stride et al., 1999). Moreover, it has been reported that Fab fragments of monoclonal antibodies QCRL-2, -3, and -4, which recognize the conformation-dependent epitopes around NH_2-proximal or COOH-proximal nucleotide-binding domain (NBD) of MRP1, inhibit the ATP-dependent transport of LTC_4 without affecting the photolabeling of MRP with 8-azido-[α-^{32}P]ATP (Hipfner et al., 1999).

The importance of the amino acid residues located in the membrane-spanning domains was previously demonstrated for MDR1 (Loo and Clarke, 1999) and CFTR (Sheppard and Welsh, 1999); e.g., alterations in amino acid residues in TM6 and 12 of MDR1 affects the function of this protein (Loo and Clarke, 1999). For CFTR, a cationic charge in the side chain at amino acid 352 (Arg), a residue flanking the predicted cytoplasmic end of the TM6 segment, is a determinant for ion selectivity in CFTR (Guinamard and Akabas, 1999). However, there has been no report concerning the amino acid residues involved in the substrate recognition/transport by MRP families. Considering the fact that the substrates for MRP families are composed of a relatively bulky hydrophobic part and a hydrophilic part possessing at least one anionic charge, charged amino acids, particularly cationic amino acids, in the membrane-spanning domain may play an important role in the recognition/transport of organic anions. To obtain insight into the interaction between MRP families and their substrates, we have used rat Mrp2 as a model protein for MRP families. In the present report, the role of charged amino acids in the membrane-spanning domain was analyzed in detail.

Experimental Procedures

Materials. [^{3}H]LTC_4 (165 Ci/mmol), [^{3}H]LTD_4 (115.3 Ci/mmol), [^{3}H]LTE_4 (146 Ci/mmol), and [^{3}H]$E_2$17βG (55 Ci/mmol) were purchased from PerkinElmer Life Science Products (Boston, MA). Unlabeled and ^{3}H-labeled DNP-SG (50.0 Ci/mmol) was synthesized enzymatically using [glycine-2-^{3}H]glutathione (PerkinElmer Life Science Products), 1-chloro-2,4-dinitrobenzene, and glutathione *S*-transferase (Sigma Chemical, St. Louis, MO) as described previously (Kobayashi et al., 1990), and the purity (>90%) was checked by thin layer chromatography. [^{14}C]E3040-glucuronide was kindly provided from Eisai Co. Ltd. (Tokyo, Japan) and [^{3}H]TLC-S (30.3 Ci/mmol) was kindly provided by Dr. Takikawa in Teikyo University (Tokyo, Japan). LTC_4, LTD_4, LTE_4, LTF_4, $E_2$17βG, ATP, AMP, creatine phosphate, and creatine phosphokinase were from Sigma Chemical. BigDye terminator was purchased from PerkinElmer (Foster City, CA). Mutagenic primers and sequencing primers were obtained from Nissinbo Industries Inc. (Tokyo, Japan). Sf9 cells were maintained as a suspension culture at 27°C with serum-free Excel 420 (Nichirei Corporation, Tokyo, Japan) supplemented with an antibiotic-antimycotic mixture (LifeTechnologies, Tokyo, Japan).

Plasmid Construction. Mrp2 in pBluescript SK(−) (Stratagene, La Jolla, CA), used previously to generate a vector for transfection of NIH3T3, included 35 nucleotides of the 5′-untranslated region of Mrp2 mRNA (Ito et al., 1998). To eliminate the potential activity of this relatively GC-rich region to reduce the translational efficiency in insect cells, the 5′ end of the Mrp2-coding sequence was amplified by polymerase chain reaction using the forward primer [5′-dcagaAGATCTaggagAGCGCTatggacaag-3′, which includes *Bgl*II (underline) and *Aor*51H I (double underline) sites] and the reverse primer (5′-dTTGGTTATAGAAGATCTCTTGG-3′). A polymerase chain reaction product of approximately 210 bases was generated and subsequently digested at the *Bgl*II sites located in the forward and reverse primer sequences. This fragment was inserted into the Mrp2 expression cassette followed by removal of the *Bgl*II fragment (one is from the multiple cloning site of the vector and the other is from the inside the Mrp2 sequence at nucleotide 171) to produce a new expression cassette Mrp2-*Aor*51H-*Sal*I. A 4.9-kilobase *Aor*51HI-*Sal*I fragment containing the full-length coding region flanked by an untranslated sequence of 3 and 222 nucleotides at the 5′ and 3′ ends, respectively, was isolated from this modified vector and connected to the *Bam*HI-*Sma*I linker at the 5′ end and subsequently inserted into the *Bam*HI and *Sal*I site of the donor plasmid pFASTBAC1 (Life Technologies) downstream from the polyhedrin promoter.

Site-Directed Mutagenesis. The *Kpn*I-*Xba*I fragment, including the 5′ end deleted Mrp2 cassette described above, was digested from the modified Mrp2/pBluescript SK(−) and subsequently inserted into the *Kpn*I-*Xba*I site of pKF18k. Mutagenesis was performed using the Mutan-Express Km site-directed mutagenesis system (Takara Shuzo Co. Ltd., Kyoto, Japan). Mutated Mrp2 was recovered as *Aor*51HI-*Sal*I fragments and ligated to *Bam*HI-*Sma*I linker at the 5′ end to be cloned into the *Bam*HI-*Sal*I site of the recombinant donor plasmid pFASTBAC1 (Life Technologies).

Production of Recombinant Baculovirus. The recombinant donor plasmids were used to transform *Escherichia coli*-competent DH10BAC cells (Life Technologies), which contain the parent bacmid and a helper plasmid. Recombinant bacmids were selected on LB plates containing 50 mg/ml kanamycin, 7 μg/ml gentamicin, 10 μg/ml tetracycline, 300 μg/ml 5-bromo-4-chloro-3-indolyl-D-galactoside, and 40 μg/ml isopropylthio-D-galactoside. The purified recombinant bacmids were transfected into Sf9 cells using CELLFECTIN Reagent (Life Technologies). Three days later, supernatant was recovered and used to infect fresh Sf9 cells. Finally, amplified virus supernatants were prepared after two cycles of this infection procedure. Their titer was determined and the virus was stored at 4°C.

Infection of Recombinant Baculovirus and Membrane Vesicle Preparation. The Sf9 cell suspension was poured into a culture dish and allowed to stand for 1 h at 27°C. During this incubation, the

cells were allowed to attach to the dish. The medium was changed to fresh medium supplemented with 5% fetal bovine serum and respective recombinant baculoviruses. In our experiments, the multiplicity of infection was 1 to 5. For control experiments, Sf9 cells were infected with a baculovirus encoding the green fluorescent protein (GFP) (GFP-control). Cells were harvested 60 to 72 h after infection and, subsequently, membrane vesicles were isolated from 1 to 2 $\times$ 10^7 Sf9 cells using the standard method described previously with some modifications (Muller et al., 1994). Briefly, cells were diluted 40-fold with hypotonic buffer (1 mM Tris-HCl, 0.1 mM EDTA, pH 7.4, at 4°C) and stirred gently for 1 h on ice in the presence of 2 mM phenylmethylsulfonyl fluoride, 5 μg/ml leupeptin, 1 μg/ml pepstatin, and 5 μg/ml aprotinin. The cell lysate was centrifuged at 100,000*g* for 30 min at 4°C, and the resulting pellet was suspended in 10 ml of isotonic TS buffer (10 mM Tris-HCl, pH 7.4 at 4°C/250 mM sucrose) and homogenized with Dounce B homogenizer (glass/glass, tight pestle, 30 strokes). The crude membrane fraction was layered on top of a 38% (w/v) sucrose solution in 5 mM Tris-HEPES, pH 7.4 at 4°C, and centrifuged in a Beckman SW41 rotor at 280,000*g* for 45 min at 4°C. The turbid layer at the interface was collected, diluted to 23 ml with TS buffer, and centrifuged at 100,000*g* for 30 min at 4°C. The resulting pellet was suspended in 400 μl of TS buffer. Vesicles were formed by passing the suspension for 30 times through a 25-gauge needle with a syringe. The membrane vesicles were finally frozen in liquid nitrogen and stored at −80°C until use. Protein concentrations were determined by the Lowry method.

Transport Study. The transport study was performed using the rapid filtration technique described previously (Ito et al., 1998). Briefly, 16 μl of transport medium [10 mM Tris, 250 mM sucrose, 10 mM $MgCl_2$, 5 mM ATP or AMP, and ATP-regenerating system (10 mM creatine phosphate, 100 μg/ml creatine phosphokinase), pH 7.4], containing radiolabeled compounds with or without unlabeled substrate, was preincubated at 37°C for 3 min and then rapidly mixed with 4 μl of membrane vesicle suspension (10 μg of protein). The transport reaction was stopped by the addition of 1 ml of ice-cold buffer containing 250 mM sucrose, 0.1 M NaCl, 10 mM Tris-HCl (pH 7.4). The stopped reaction mixture was filtered through a 0.45-μm HVWP filter (Millipore Corp., Bedford, MA) and then washed twice with 5 ml of stop solution. Radioactivity retained on the filter was determined using a liquid scintillation counter (LSC-3500; Aloka Co., Tokyo, Japan).

The initial uptake rate of a tracer amount of each ligand was determined in the presence of ATP or AMP; [^{3}H]DNP-SG (55 nM at 5 min), [^{3}H]LTC_4 (1.7 nM at 1 min), [^{3}H]$E_2$17βG (50 nM at 2 min), [^{3}H]E3040-glucuronide (20 μM at 5 min), [^{3}H]TLC-S (16.5 nM at 5 min). The relative transport activity of each ligand by mutant Mrp2 was calculated by subtracting the uptake into vesicles containing GFP from that into vesicles containing the mutant Mrp2 in the presence of ATP. This is possible because the same transport activity was observed in the absence of ATP in both GFP- and Mrp2-expressing vesicles (data not shown).

The relative uptake (R_{rel}) rate was calculated for each ligand using the equation R_{rel} = ($Uptake_{mut}$ − $Uptake_{GFP}$) / ($Uptake_{wild\ type}$ − $Uptake_{GFP}$), where $Uptake_{mut}$, $Uptake_{wild\ type}$, and $Uptake_{GFP}$ represent the initial uptake rate (pmol/min/mg) of each ligand into mutant Mrp2s, wild-type Mrp2, and GFP-containing vesicles in the presence of ATP, respectively. The calculated R_{rel} values were then normalized using the equation R′ = R_{rel} (ligand) / R_{rel} ($E_2$17βG), where R_{rel} (ligand) represents the R_{rel} value for each ligand (TLC-S, DNP-SG, LTC_4, and E3040-glucuronide), and R_{rel} ($E_2$17βG) represents the R_{rel} value for $E_2$17βG. Thus, R′ represents the relative transport activity of each ligand into the wild-type and mutant Mrp2-expressing vesicles normalized with respect to the transport of $E_2$17βG into the respective membrane vesicles. In the present report, the results of the transport studies are given as the mean ± S.E. with the number of determinations unless otherwise noted.

Western Blot Analysis. Membrane vesicles from Sf9 cells were loaded on to a 8.5% polyacrylamide slab gel containing 0.1% SDS and then transferred on to a Pall Fluoro Trans W membrane filter (Pall Gelman Sciences, Ann Arbor, MI) by electroblotting. The filter was blocked with Tris-buffered saline containing 0.05% Tween 20 and 5% bovine serum albumin for 2 h at room temperature and probed overnight at room temperature with polyclonal anti-Mrp2 antibody raised against the upstream region of carboxyl-terminal NBD (amino acid residues 1272–1285) (CP-2 antibody, supplied by Dr. Nakayama in Kumamoto University, Kumamoto, Japan) diluted with Tris-buffered saline containing 0.05% Tween 20 and 0.5% bovine serum albumin (1:1000). Antibody was visualized with ^{125}I-anti-rabbit antibody (Amersham Pharmacia Biotech, Uppsala, Sweden), followed by exposure to Fuji imaging plates (Fuji Photo Film Co., Ltd., Kanagawa, Japan) for 3 h at room temperature, and analyzed with an imaging analyzer (BAS 1500; Fuji Photo Film Co., Ltd.).

Results

Charged Amino Acids in the Transmembrane Domains Conserved in the MRP Family. Human MRP1 is composed of 17 TM helices to form three membrane-spanning domains (MSD1, 2, and 3) connected by poorly conserved linker regions (L_0 and L_1) and highly conserved nucleotide binding domains (NBD1 and NBD2) (Bakos et al., 1996; Hipfner et al., 1997). A hydropathy plot analysis of rat Mrp2 with the Kite & Doolittle algorithm suggested a similar profile to that of human MRP1. Moreover, similar profiles were obtained for other MRP members, including mouse Mrp1 (Stride et al., 1996), human (Taniguchi et al., 1996) and rabbit MRP2 (van Aubel et al., 1998), and human (Kool et al., 1997; Kiuchi et al., 1998) and rat MRP3 (Hirohashi et al., 1998). A schematic diagram illustrating the structure is shown in Fig. 1A and this was predicted from the hypothesis that rat Mrp2 also has the same membrane topology and domain organization as human MRP1. To determine the key amino acid residues for recognition and/or transport of organic anions via MRP families, the charged amino acids in the transmembrane domains of rat Mrp2 were examined first. Because it is difficult to predict whether amino acids are located inside or outside the lipid bilayer at the boundary, we selected 47 cationic amino acids (i.e., Lys, Arg, and His) within and/or around the TM of rat Mrp2. Alignment of the extended TMs (TM6, 11, 13, 14, 16, and 17), in which conserved charged amino acids were found, is shown in Fig. 1B. Among them, cationic amino acids, Arg or Lys at 308 and 325 (TM6), 586 (TM11), 1019 (TM13), 1201 (TM16), and 1226 (TM17), were found to be conserved among MRP1–3. The transport properties of MRP1 and 2 are different from those of Mrp3 in that the former accept both glutathione conjugates and glucuronide conjugates as good substrates (Suzuki and Sugiyama, 1998; Cui et al., 1999), whereas the latter accepts only glucuronide conjugates as good substrates (Hirohashi et al., 1999). The difference in the substrate specificity of these MRP families prompted us to find additional two cationic amino acids at 1096 (TM14) and 1206 (TM16), which are conserved in MRP1 and 2, but not in MRP3. Moreover, anionic amino acids conserved in MRP1–3 were found at 329 (TM6) and 1208 (TM16).

Site-directed mutagenesis was performed on these 10 charged amino acids, which are partially or fully conserved among the MRP families. Moreover, the cationic amino acid at 320 (TM6), which was found only in MRP2, was selected as a negative control for this site-directed mutagenesis analysis.

In the present study, cationic amino acids substituted by

Met resulted in the production of the corresponding mutant Mrp2s. These include K308M, K320M, K325M, R1019M, R1201M, R1206M, and R1226M. For R586 and R1096, Arg was substituted by Leu (R586L and R1096L). The anionic amino acid residues Asp at 329 and Glu at 1208 were substituted by the corresponding neutral amino acids to produce D329N and E1208Q, respectively. In addition, we have introduced further extensive mutations in Mrp2 cDNA, such as K325R, R586K, and R586I, and D329E to assess the effect of substitution by other amino acids in these positions.

Expression of Wild-Type and Mutant Mrp2 in Sf9 Cells. The expression of a series of mutant Mrp2s in the infected cells was confirmed by Western blot analysis. The antibody recognized an ~190-kDa band in the membrane vesicles from Sprague-Dawley rat liver (data not shown). Slightly shorter bands of ~175 kDa were detected in membrane vesicles isolated from Sf9 cells infected with wild-type or mutant Mrp2 cDNA carrying baculoviruses, but not in GFP-control vesicles (Fig. 2). The difference in the molecular mass may be accounted for by the lower degree of sugar modification in the insect cells, as reported for rabbit Mrp2 expressed in Sf9 cells (van Aubel et al., 1998).

Densitometric analysis revealed up to 12-fold difference in the expression levels among mutant Mrp2s, except for R1201M and R1226M, whose expression was below the limit of detection. Alteration of the translational efficiency and/or stability of the protein caused by the amino acid substitution may be one reason for the difference in expression level between mutant Mrp2s.

Transport of Mrp2 Substrates into Membrane Vesicles from Sf9 Cells. Previously described Mrp2 substrates were subjected to an analysis of their transport activity. ATP-dependent uptake of typical substrates for Mrp2 into wild-type Mrp2-expressing membrane vesicles was significantly enhanced compared with GFP-control vesicles; [^{3}H]TLC-S [495 ± 91.5 versus 65 ± 2.7 μl/mg/min at 40 nM; $n = 3$ ($p < 0.01$)], [^{3}H]DNP-SG [15.1 ± 2.2 versus 2.1 ± 1.8 μl/mg/min at 55 nM; $n = 3$ ($p < 0.05$)], [^{3}H]LTC$_4$ [1430 ± 3.6 versus 67 ± 8.1 μl/mg/min at 1.7 nM; $n = 3$ ($p < 0.01$)], [^{3}H]E3040-glucuronide [19.3 ± 1.4 versus 2.6 ± 0.05 μl/mg/min at 6.5 μM; $n = 3$ ($p < 0.01$)], and [^{3}H]E$_2$17βG [75.0 ± 3.1 versus 7.9 ±1.0 μl/mg/min at 50 nM; $n = 3$ ($p < 0.01$)].

Alterations in the substrate specificity were found in some mutant Mrp2s (Fig. 3). The relative transport activities (R′ values) of all compounds examined were not affected in K308M, K320M, and R1096L compared with the wild-type Mrp2 (Fig. 3). Mrp2-dependent transport of all substrates was not detectable in R1206M and E1208Q (data not shown), whereas adequate expression of these mutated Mrp2 molecules was demonstrated in the Western blot (Fig. 2). Most interestingly, a marked reduction in the relative transport activity for DNP-SG and LTC$_4$ transport was observed in K325M and R586L, whereas those for E3040-glucuronide and TLC-S were not significantly different from those in wild-type Mrp2 (Fig. 3). Although the absolute transport activity for E$_2$17βG, E3040-glucuronide and TLC-S decreases to some extent in D329N (data not shown), relatively greater reduction in the transport activity for glutathione conjugates was observed in D329N (Figs. 3 and 8).

Concentration Dependence of E$_2$17βG and DNP-SG Uptake. To determine the changes in the affinity of glutathione and glucuronide conjugates for K325M and R586L, whose transport activity of glutathione conjugates was significantly reduced (Fig. 3), the concentration dependence in the transport of E$_2$17βG and DNP-SG was determined. The initial uptake rate of each compound was determined at several concentrations of E$_2$17βG (0.1–75 μM) and DNP-SG (2.4–600 μM) and was used to calculate the K_m values for wild-type Mrp2, K325M, and R586L (Fig. 4; Table 1). The K_m values for wild-type Mrp2, K325M, and R586L-mediated transport of E$_2$17βG were 3.91 ± 0.93, 0.40 ± 0.05, and 1.40 ± 0.46 μM (mean ± computer calculated S.D.), respec-

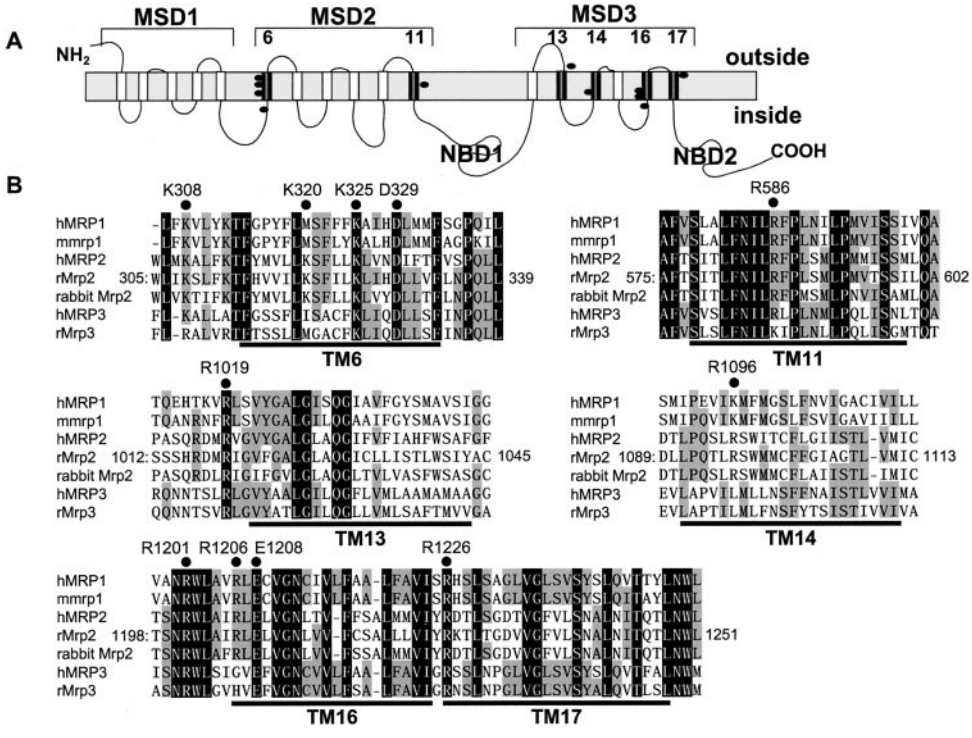

Fig. 1. Membrane topology of Mrp2 and alignment of transmembrane domains of MRP families. A, membrane topology of Mrp2 was predicted by the Kite & Doolittle algorithm, taking into account the reported model for MRP1 (Bakos et al., 1996; Hipfner et al., 1997). Dots represent the approximate location of amino acid residues that underwent site-directed mutagenesis. B, detailed alignment of TM of Mrp2 with respective TM number is shown in comparison with human and mouse MRP1; human, rat, and rabbit MRP2; and human and rat MRP3. The amino acid number is shown only for rat Mrp2. Predicted TMs are underlined. Dots represent the location of amino acid residues where mutation was introduced.

tively (Fig. 4A; Table 1). The K_m values of DNP-SG were 80.8 ± 7.0 and 308 ± 51 μM (mean ± computer calculated S.D.) for wild-type Mrp2 and R586L, respectively (Fig. 4B; Table 1). No kinetic parameters could be determined for K325M, due to the extremely low transport activity of [^{3}H]DNP-SG.

Mutual Inhibition of DNP-SG and $E_2$17βG. To determine whether the changes in the inhibitory potency of $E_2$17βG and DNP-SG were associated with changes in the K_m values in mutant Mrp2s, the mutual inhibitory effect of these two conjugates was examined. The IC_{50} values of $E_2$17βG for the uptake of [^{3}H]DNP-SG were 13.3 ± 2.3 and 2.30 ± 1.2 μM (mean ± computer calculated S.D.) for wild-type Mrp2 and R586L, respectively (Fig. 5A; Table 1), whereas the IC_{50} values of DNP-SG for the uptake of [^{3}H]$E_2$17βG were 19.3 ± 3.5, 360 ± 89, and 59.5 ± 9.8 μM (mean ± computer calculated S.D.) for wild-type Mrp2, K325M, and R586L, respectively (Fig. 5B; Table 1). Because tracer concentrations of isotopically labeled ligands were used in the present study, these IC_{50} values represent the respective K_i values. The increase in the affinity of $E_2$17βG for R586L and the reduction in the affinity of DNP-SG for both K325M and R586L were also confirmed in these mutual inhibition experiments (Fig. 5; Table 1).

Structural Requirement for the Recognition of Glutathione Conjugate. To obtain insight into the relationship between structural differences in the glutathione moiety and the transport activity, the inhibitory effect of a series of leukotriene derivatives on the uptake of $E_2$17βG was studied in wild-type Mrp2, K325M, and R586L. In wild-type Mrp2, the uptake of a tracer amount of [^{3}H]$E_2$17βG (55 nM) was inhibited in a concentration-dependent manner by LTC_4 with an IC_{50} value of 0.65 ± 0.12 μM (mean ± computer calculated S.D.; Table 2), which was similar to the K_m value for LTC_4 in wild-type Mrp2 [0.38 ± 0.06 μM (mean ± computer calculated S.D.); data not shown]. The inhibitory potency of LTC_4 was significantly reduced in K325M, with an apparent IC_{50} value of 16.0 ± 9.0 μM (mean ± computer calculated S.D.), in accordance with the reduced transport activity for LTC_4 in the mutant Mrp2 (Fig. 3). In contrast, the inhibitory potency was not significantly altered in K325M and R586L for other leukotriene derivatives, including LTD_4, LTE_4, and LTF_4, and MK571 (Table 2). Also, the ATP-dependent transport of LTC_4 was lost in both mutant Mrp2s, although those of LTD_4 and LTE_4 in mutant Mrp2s remained to significant levels (Fig. 7).

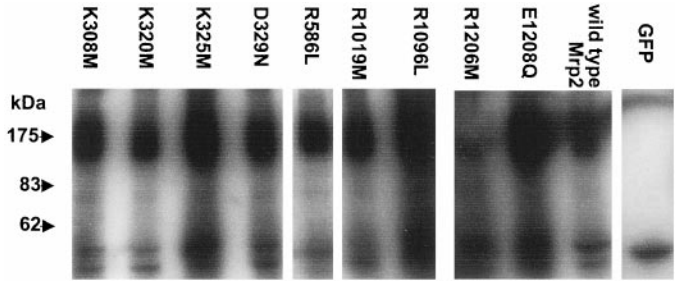

Fig. 2. Western blot analysis of wild-type and mutant Mrp2s. Membrane vesicles (50 μg of protein) were separated on an 8.5% polyacrylamide slab gel containing 0.1% SDS. The fractionated proteins were transferred on to a membrane filter by electroblotting and wild-type and mutant Mrp2s were detected by polyclonal anti-Mrp2 antiserum.

Compensation of the Charged Amino Acid at 325, 329, and 586. To further examine the requirement of charged amino acids at 325, 329, and 586 for the transport activity of glutathione conjugates, we constructed K325R, D329E, R586K, and R586I. The expression level of mutant Mrp2 proteins was similar among these mutant Mrp2s and wild-type Mrp2 (data not shown). ATP-dependent uptake of [^{3}H]$E_2$17βG was detected in these mutant Mrp2s, although

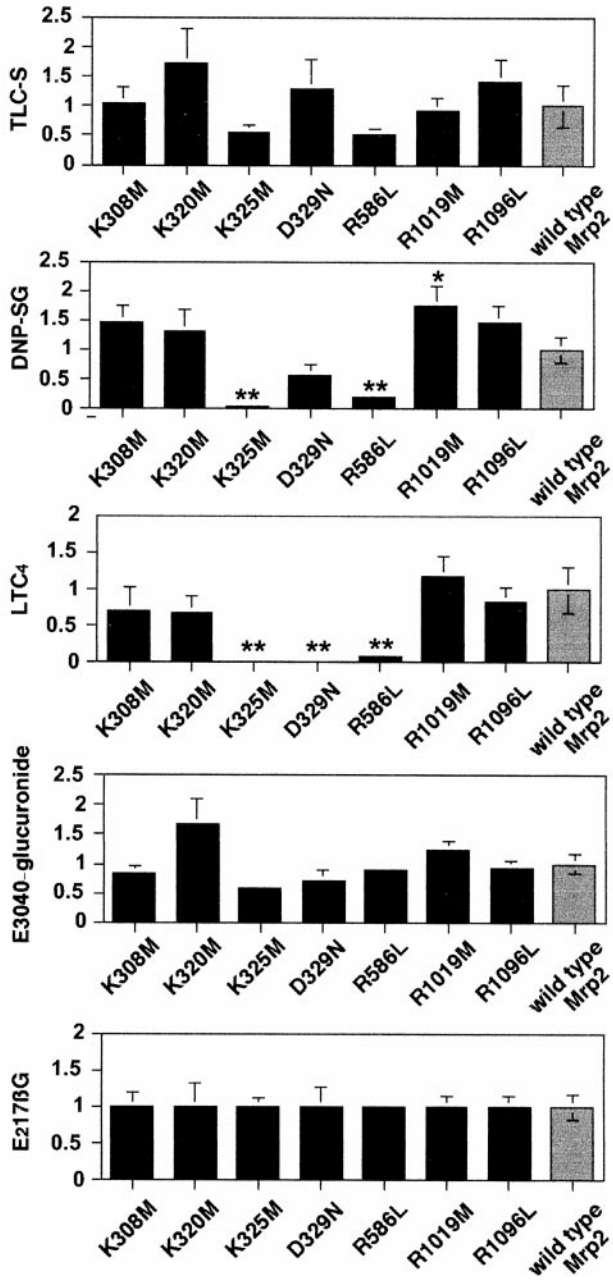

Fig. 3. Uptake of Mrp2 substrates by wild-type and mutant Mrp2s. ATP-dependent uptake of [^{3}H]TLC-S (16.5 nM at 5 min), [^{3}H]DNP-SG (55 nM at 2 min), [^{3}H]LTC_4 (1.7 nM at 1 min), [^{3}H]E3040-glucuronide (20 μM at 5 min), and [^{3}H]$E_2$17βG (50 nM at 2 min) into membrane vesicles expressing wild-type and mutant Mrp2 is shown. Amounts of 2 to 10 μg of membrane vesicles were used for transport experiments at 37°C in the presence of ATP or AMP. Results are shown as the relative transport activity normalized by $E_2$17βG transport (R′ value; see *Experimental Procedures*). Each column represents the mean ± S.E. of triplicate determinations. N.D., not detectable. *$p < 0.05$ and **$p < 0.01$, significantly different from wild-type Mrp2 by ANOVA followed by Dunnett's test.

the absolute values were not identical among these mutant Mrp2s and wild-type Mrp2 (Fig. 8). In contrast, the ATP-dependent uptake of [^{3}H]LTC_4 and [^{3}H]DNP-SG relative to that of [^{3}H]$E_2$17βG was reduced in K325R, K325M, R586I, R586L, D329E, and D329N, whereas no reduction was observed in R586K (Fig. 8).

Discussion

Although the results of previous transport studies with isolated bile canalicular membrane vesicles (CMVs) and membrane vesicles expressing Mrp2 indicated that both of the glutathione conjugates and glucuronide conjugates are substrates for Mrp2 (Keppler and Konig, 1997; Suzuki and Sugiyama, 1998), there was no direct evidence showing that these conjugates were indeed recognized by exactly the same recognition site. In the present study, we examined the mechanism for the transport/recognition of ligands by using the membrane vesicles isolated from Sf9 cells expressing the wild-type and mutant Mrp2s, particularly focusing on the role of charged amino acids located in the transmembrane domains. Transport activity of ligands by mutant Mrp2s was shown as the relative transport activity (R′) after normalization by that of $E_2$17βG; although it is better to normalize the uptake values in terms of the expression levels of mutant Mrp2 proteins, it is difficult to quantitatively determine the protein levels in an exact manner by Western blot analyses. Because our major purpose is to see the change in the substrate specificity of rat Mrp2 between glutathione conjugates and glucuronide conjugates, the uptake values of each ligand were normalized in terms of the uptake values of a standard compound. As a standard compound, we chose $E_2$17βG, because this compound is transported even by some of the mutant Mrp2s (K325M, D329N, and R586L), which do not transport glutathione conjugates. However, this normalization does not necessarily correct for the expression levels of mutant Mrp2 proteins, because the uptake of $E_2$17βG is affected not only by the protein levels but also by the kinetic parameters for $E_2$17βG (Table 1). After this normalization, we found a selective loss of transport activity for glutathione conjugates in K325M and R586L (Fig. 3), whereas an increase in the affinity for glucuronide conjugates was observed in these mutant Mrp2s (Figs. 4 and 5). Collectively, it was suggested that glutathione conjugates and glucuronide conjugates are not necessarily recognized by the same mechanism. These results are consistent with the observations in the kinetic studies; e.g., the IC_{50} values of DNP-SG on the transport of $E_2$17βG are different from K_m values of DNP-SG for both of wild-type and mutant Mrp2 (R586L) (Table 1).

The results shown in Figs. 3, 7, and 8 suggest that the amino acid residues at 325 and 586 play an important role in discriminating each conjugate. The fact that the transport activity for LTC_4 is maintained in R586K, but not in R586L or R586I (Fig. 8), indicates the requirement for a cationic charge at 586 to be able to recognize glutathione conjugates. In contrast, Arg and Glu could not compensate for the function of Lys at 325 and Asp at 329, respectively. These results demonstrate that functional compensation by cationic amino

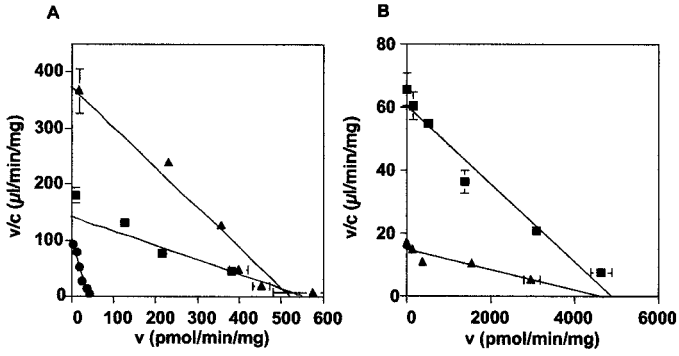

Fig. 4. Eadie-Hofstee plot for the uptake of $E_2$17βG and DNP-SG. Saturable uptake of [^{3}H]$E_2$17βG (55 nM; A) and [^{3}H]DNP-SG (50 nM; B) was examined at 37°C in membrane vesicles expressing wild-type Mrp2 (■), K325M (●), and R586L (▲). Each symbol represents the Mrp2-dependent uptake determined by subtracting the uptake into GFP-control vesicles from that into Mrp2-expressing vesicles in the presence of ATP. Each point and bar represents the mean ± S.E. of triplicate determinations.

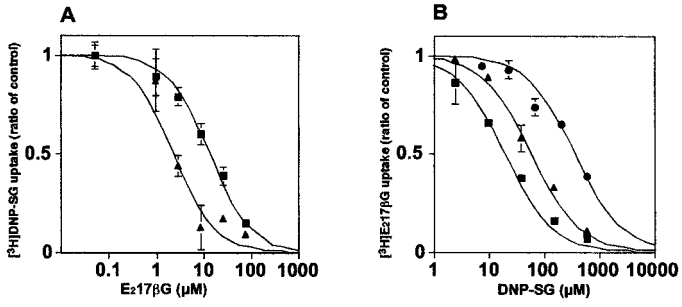

Fig. 5. Mutual inhibition between Mrp2-mediated transport of $E_2$17βG and DNP-SG. The effect of $E_2$17βG on the uptake of [^{3}H]DNP-SG (50 nM; A) and effect of DNP-SG on the uptake of [^{3}H]$E_2$17βG (55 nM; B) were examined at 37°C in membrane vesicles expressing wild-type Mrp2 (■), K325M (●), and R586L (▲). The Mrp2-dependent uptake was obtained by subtracting the uptake into GFP-control vesicles from that into Mrp2-expressing vesicles in the presence of ATP. Results are given as a ratio to the values determined in the absence of unlabeled compounds. Each point and vertical bar represents the mean ± S.E. of triplicate determinations.

TABLE 1

Kinetic parameters for the transport of DNP-SG and $E_2$17βG by wild-type Mrp2, K325M, and R586L

K_m and IC_{50} values were calculated on the basis of the data shown in Figs. 4 and 5, respectively. Each represents the obtained parameter ± computer calculated S.D. Comparison of K_m values for $E_2$17βG and DNP-SG, respectively, was performed by ANOVA followed by Dunnett's test, whereas that of IC_{50} and K_m values for $E_2$17βG and DNP-SG, respectively, was performed by Student's t test.

	$E_2$17βG		DNP-SG	
	K_m	IC_{50}	K_m	IC_{50}
	μM		μM	
Wild-type Mrp2	3.91 ± 0.93	13.3 ± 2.3¶¶	80.8 ± 7.0	19.3 ± 3.5¶¶¶
K325M	0.40 ± 0.05**	N.D.	N.D.	360 ± 89**
R586L	1.40 ± 0.46**	2.30 ± 1.17**	308 ± 51**	59.5 ± 9.8¶¶

N.D., not determined.
** $p < 0.01$, significantly different from wild-type Mrp2.
¶¶ $p < 0.01$ and ¶¶¶ $p < 0.001$, significantly different from respective K_m value.

acid is possible at Arg 586, but not at Lys 325. In addition, Glu 329 was not functionally substituted by anionic amino acid. These results may be accounted for by the hypothesis that these cationic and anionic amino acids are necessary parts of the functional structure for the recognition/transport of glutathione conjugates. Another possible hypothesis is that the cationic side chain of amino acid residues may interact directly with the anionic charge of glutathione conjugates. The former hypothesis has already been proposed for many membrane proteins, including transporters and ion channels (Merickel et al., 1997; Gupta et al., 1998). For example, the salt bridge between Lys in TM2 and Asp in TM11 of the vesicular monoamine transporter has been shown to be important for transport activity (Merickel et al., 1997). Substitution of either Lys by Ala or Asp by Ala resulted in the loss of transport activity for monoamines (Merickel et al., 1997). The same mechanism may hold for Mrp2; in Mrp2, Asp at 329 is adjacent to Lys at 325 at intervals of four amino acid residues in the same transmembrane helices (TM6). Interaction of the side chains of K325 and D329 is plausible, because a hydrogen bond can be formed between the carbonyl oxygen and amino hydrogen of the amino acids at position n and n + 4 in an α-helix. This hypothesis is further supported by the fact that both K325M and D329N lost transport activity for glutathione conjugates, but not for other conjugates (Fig. 3). Similar conformational changes may have occurred in these two mutant Mrp2s due to the disappearance of a salt bridge between K325 and D329. Although R586 plays a critical role in transporting glutathione conjugates (Fig. 3), there is no candidate anionic amino acid able to form a salt bridge around R586 in the same helix. Interaction with distant amino acid residues in another transmembrane helix or direct interaction with the anionic charge of the ligand molecule may be one of the roles of R586.

Recently, Stride et al. (1999) described the importance of the carboxyl-terminal domain of MRP1 in the transport of $E_2 17\beta G$ using chimeric protein of human and mouse MRP1. They suggested that the recognition site for LTC_4 and $E_2 17\beta G$ in MRP1 is not absolutely equivalent, based on the finding that comparable transport activity for LTC_4 is observed in wild type and a series of MRP1 chimeras, whereas the extent of transport of $E_2 17\beta G$ was very different among mutants (Stride et al., 1999). No information about the recognition site for the glutathione conjugate was obtained from the human and mouse MRP1 chimera studies, because sim-

TABLE 2

IC_{50} values of cysteinyl leukotriene derivatives on the uptake of $[^3H]E_2 17\beta G$

The effect of a series of cysteinyl leukotrienes on the uptake of $[^3H]E_2 17\beta G$ (55 nM) was examined at 37°C in membrane vesicles expressing wild-type Mrp2, K325M, and R586L. The IC_{50} values were calculated by subtracting the uptake into GFP-control vesicles from that of Mrp2-expressing vesicles. Each represents the obtained parameter ± computer-calculated S.D.

IC_{50}	Wild-Type Mrp2	K325M	R586L
μM			
LTC_4	0.65 ± 0.12	16.0 ± 9.0*	5.95 ± 4.2
LTD_4	5.48 ± 0.98	11.0 ± 3.4	13.1 ± 5.9
LTE_4	9.83 ± 1.4	14.7 ± 4.2	4.83 ± 1.3
LTF_4	10.0 ± 4.6	15.2 ± 5.9	9.27 ± 2.7
MK571	2.62 ± 1.1	3.26 ± 0.88	2.50 ± 0.69

* $p < 0.05$, significantly different from wild-type Mrp2 by ANOVA followed by Dunnett's test.

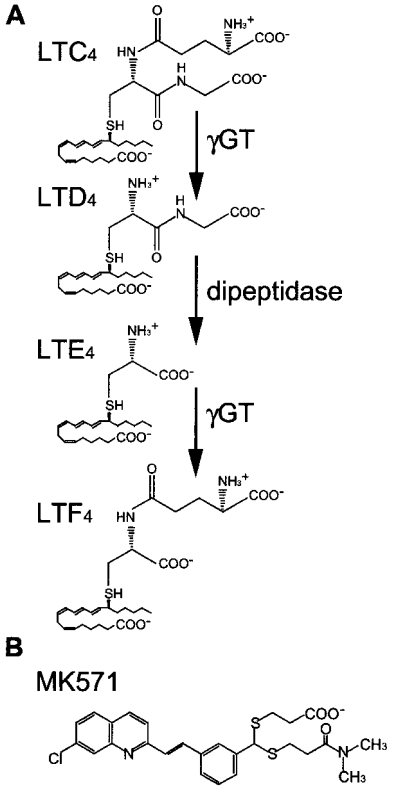

Fig. 6. Structure and metabolic pathway of cysteinyl leukotrienes. A, structure and schematic pathway of LTC_4. B, structure of MK571.

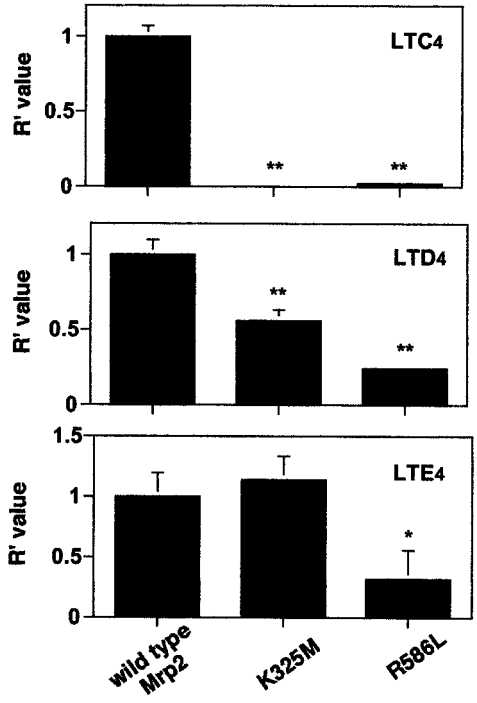

Fig. 7. Uptake of cysteinyl leukotriene derivatives by wild-type and mutant Mrp2. The uptake of $[^3H]LTC_4$ (1.7 nM), $[^3H]LTD_4$ (11 nM), and $[^3H]LTE_4$ (8.6 nM) was examined at 37°C in membrane vesicles expressing wild-type Mrp2, K325M, and R586L in the presence of AMP and ATP. Results are shown as the relative transport activity normalized by $E_2 17\beta G$ transport (R′ value; see *Experimental Procedures*). Each column represents the mean ± S.E. of triplicate determinations. N.D., not detectable. * $p < 0.05$ and ** $p < 0.01$, significantly different from wild-type Mrp2 by ANOVA followed by Dunnett's test.

ilar transport activity for LTC_4 was observed in both orthologs (Stride et al., 1999). Our results are the first demonstration of the importance of TM6 and TM11, particularly the charged amino acids in these helices, for the recognition/transport of the glutathione conjugate. However, we cannot determine the requirement of other amino acid residues, as far as the function of Mrp2 is concerned, due to the limitations in the site-directed mutagenesis approach. Chimeric studies between Mrp2 and Mrp3 would provide an answer to this question.

The mechanism of substrate recognition was further investigated using a series of leukotriene derivatives. As shown in Fig. 6, LTD_4, LTE_4, and LTF_4 are the sequential metabolites of LTC_4; LTD_4 is the metabolite of LTC_4 produced by γ-glutamyl transpeptidase, containing the Cys-Gly-conjugate structure. LTE_4 is the metabolite produced from LTD_4 by dipeptidase, containing the Cys-conjugate structure (Fig. 6). Finally, LTF_4 is produced from LTE_4 by γ-glutamyl transpeptidase to form Glu-Cys-conjugate structure (Fig. 6). In addition, MK571 is an analog of LTD_4 (Fig. 6). Using rat CMVs, the transport activity of LTD_4 and LTE_4 was determined to be 46 and 11% that of LTC_4, respectively (Ishikawa et al., 1990). This is also compatible with the rank order of MRP1-mediated transport (Jedlitschky et al., 1996). LTD_4 and LTE_4 were also transported into wild-type Mrp2-expressing membrane vesicles in an ATP-dependent manner (Fig. 7). The initial velocity of the uptake of LTD_4 and LTE_4 by wild-type Mrp2 was 7.4 ± 0.3 and 1.8 ± 0.1% (mean ± S.E., $n = 3$) that of LTC_4, respectively (Fig. 7), which was one-sixth of those reported in CMVs (Ishikawa et al., 1990).

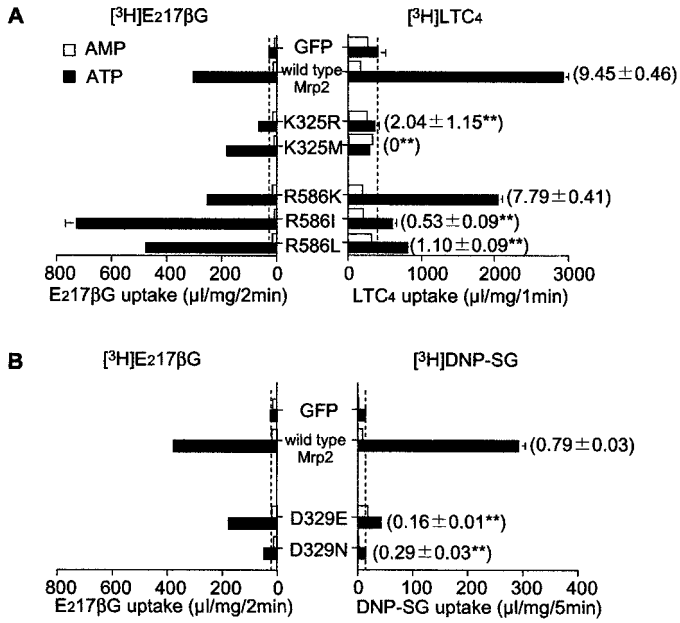

Fig. 8. Uptake of glutathione conjugates by conservative mutant Mrp2s for K325, R586, and D329. A, uptake of [^{3}H]$E_2$17βG (55 nM at 2 min) and [^{3}H]LTC_4 (1.7 nM at 1 min) was examined at 37°C in membrane vesicles expressing wild-type Mrp2, K325R, K325M, R586K, R586I, and R586L in the presence of AMP (open bar) and ATP (closed bar). B, uptake of [^{3}H]$E_2$17βG (55 nM at 2 min) and [^{3}H]DNP-SG (50 nM at 5 min) was examined at 37°C in membrane vesicles expressing wild-type Mrp2, D329E, and D329N in the presence of AMP (open bar) and ATP (closed bar). Numbers in parentheses represent the transport activities of glutathione conjugates relative to that of [^{3}H]$E_2$17βG (mean ± S.E. of triplicate determinations). $^{**}p < 0.01$, significantly different from wild-type Mrp2 by ANOVA followed by Dunnett's test.

The inhibition constants (IC_{50}) of LTD_4 and LTE_4 for the uptake of $E_2$17βG into wild-type Mrp2 [5.48 ± 0.98 and 9.83 ± 1.4 μM (mean ± calculated S.D.), respectively (Table 2)] were similar to the previously reported K_m values in CMVs (1.5 and >10 μM, respectively) (Ishikawa et al., 1990). Although there is no published information on the affinity of LTF_4 for MRP families, LTF_4 has a low inhibitory potency as LTD_4 and LTE_4, compared with LTC_4 (Table 2). The IC_{50} values of these LT derivatives, except for LTC_4, were similar in K325M, R586L, and wild-type Mrp2 (Table 2). Together with the finding that the transport activity for LTD_4 and LTE_4, but not for LTC_4, was retained in K325M and K586L (Fig. 7), these results indicate a difference in the mechanism of recognition/transport by Mrp2 among LTC_4 and its sequential metabolites. Moreover, the cationic side-chains of K325 or R586 may not directly interact with the anionic charges of glutamic acid or glycine of the intact glutathione moiety, or those of glucuronide or sulfate conjugates.

In conclusion, we have demonstrated the important role played by charged amino acid residues in TM6 and TM11 for the transport of glutathione conjugates. These findings provide important information about the transport mechanism of MRP families. While this article was being considered for publication, Ryu et al. (2000) independently indicated that several charged amino acids in human MRP2 TM domains are involved in the transport activity of glutathione methyfluorescein.

References

Bakos E, Evers R, Szakacs G, Tusnady GE, Welker E, Szabo K, de Haas M, van Deemter L, Borst P, Varadi A, et al. (1998) Functional multidrug resistance protein (MRP1) lacking the N-terminal transmembrane domain. *J Biol Chem* **273:**32167–32175.

Bakos E, Hegedus T, Hollo Z, Welker E, Tusnady GE, Zaman GJ, Flens MJ, Varadi A and Sarkadi B (1996) Membrane topology and glycosylation of the human multidrug resistance-associated protein. *J Biol Chem* **271:**12322–12326.

Büchler M, König J, Brom M, Kartenbeck J, Spring H, Horie T and Keppler D (1996) cDNA cloning of the hepatocyte canalicular isoform of the multidrug resistance protein, cMrp, reveals a novel conjugate export pump deficient in hyperbilirubinemic mutant rats. *J Biol Chem* **271:**15091–15098.

Cole SP and Deeley RG (1998) Multidrug resistance mediated by the ATP-binding cassette transporter protein MRP. *Bioessays* **20:**931–940.

Cui Y, König J, Buchholz JK, Spring H, Leier I and Keppler D (1999) Drug resistance and ATP-dependent conjugate transport mediated by the apical multidrug resistance protein, MRP2, permanently expressed in human and canine cells. *Mol Pharmacol* **55:**929–937.

Deeley RG and Cole SP (1997) Function, evolution and structure of multidrug resistance protein (MRP). *Semin Cancer Biol* **8:**193–204.

Evers R, Kool M, van Deemter L, Janssen H, Calafat J, Oomen LC, Paulusma CC, Oude Elferink RP, Baas F, Schinkel AH, et al. (1998) Drug export activity of the human canalicular multispecific organic anion transporter in polarized kidney MDCK cells expressing cMOAT (MRP2) cDNA. *J Clin Invest* **101:**1310–1319.

Gao M, Loe DW, Grant CE, Cole SPC and Deeley RG (1996) Reconstitution of ATP-dependent leukotriene C4 transport by co-expression of both half-molecules of human multidrug resistance protein in insect cells. *J Biol Chem* **271:**27782–27787.

Gao M, Yamazaki M, Loe DW, Westlake CJ, Grant CE, Cole SP and Deeley RG (1998) Multidrug resistance protein. Identification of regions required for active transport of leukotriene C4. *J Biol Chem* **273:**10733–10740.

Guinamard R and Akabas MH (1999) Arg352 is a major determinant of charge selectivity in the cystic fibrosis transmembrane conductance regulator chloride channel. *Biochemistry* **38:**5528–5537.

Gupta SS, DeWitt ND, Allen KE and Slayman CW (1998) Evidence for a salt bridge between transmembrane segments 5 and 6 of the yeast plasma-membrane H+-ATPase. *J Biol Chem* **273:**34328–34334.

Hipfner DR, Almquist KC, Leslie EM, Gerlach JH, Grant CE, Deeley RG and Cole SP (1997) Membrane topology of the multidrug resistance protein (MRP). A study of glycosylation-site mutants reveals an extracytosolic NH2 terminus. *J Biol Chem* **272:**23623–23630.

Hipfner DR, Mao Q, Qiu W, Leslie EM, Gao M, Deeley RG and Cole SP (1999) Monoclonal antibodies that inhibit the transport function of the 190-kDa multidrug resistance protein, MRP. Localization of their epitopes to the nucleotide-binding domains of the protein. *J Biol Chem* **274:**15420–15426.

Hirohashi T, Suzuki H, Ito K, Ogawa K, Kume K, Shimizu T and Sugiyama Y (1998) Hepatic expression of multidrug resistance-associated protein-like proteins maintained in Eisai hyperbilirubinemic rats. *Mol Pharmacol* **53:**1068–1075.

Hirohashi T, Suzuki H and Sugiyama Y (1999) Characterization of the transport

properties of cloned rat multidrug resistance-associated protein 3 (MRP3). *J Biol Chem* **274:**15181–15185.
Ishikawa T, Muller M, Klunemann C, Schaub T and Keppler D (1990) ATP-dependent primary active transport of cysteinyl leukotrienes across liver canalicular membrane. Role of the ATP-dependent transport system for glutathione S-conjugates. *J Biol Chem* **265:**19279–19286.
Ito K, Suzuki H, Hirohashi T, Kume K, Shimizu T and Sugiyama Y (1997) Molecular cloning of canalicular multispecific organic anion transporter defective in EHBR. *Am J Physiol* **272:**G16–G22.
Ito K, Suzuki H, Hirohashi T, Kume K, Shimizu T and Sugiyama Y (1998) Functional analysis of a canalicular multispecific organic anion transporter cloned from rat liver. *J Biol Chem* **273:**1684–1688.
Jedlitschky G, Leier I, Buchholz U, Barnouin K, Kurz G and Keppler D (1996) Transport of glutathione, glucuronate, and sulfate conjugates by the MRP gene-encoded conjugate export pump. *Cancer Res* **56:**988–994.
Kartenbeck J, Leuschner U, Mayer R and Keppler D (1996) Absence of the canalicular isoform of the MRP gene-encoded conjugate export pump from the hepatocytes in Dubin-Johnson syndrome. *Hepatology* **23:**1061–1066.
Keppler D and König J (1997) Hepatic canalicular membrane 5: expression and localization of the conjugate export pump encoded by the MRP2 (cMRP/cMOAT) gene in liver. *FASEB J* **11:**509–516.
Kiuchi Y, Suzuki H, Hirohashi T, Tyson CA and Sugiyama Y (1998) cDNA cloning and inducible expression of human multidrug resistance associated protein 3 (MRP3). *FEBS Lett* **433:**149–152.
Kobayashi K, Sogame Y, Hara H and Hayashi K (1990) Mechanism of glutathione S-conjugate transport in canalicular and basolateral rat liver plasma membranes. *J Biol Chem* **265:**7737–7741.
König J, Rost D, Cui Y and Keppler D (1999) Characterization of the human multidrug resistance protein isoform MRP3 localized to the basolateral hepatocyte membrane. *Hepatology* **29:**1156–1163.
Kool M, de Haas M, Scheffer GL, Scheper RJ, van Eijk MJ, Juijn JA, Baas F and Borst P (1997) Analysis of expression of cMOAT (MRP2), MRP3, MRP4, and MRP5, homologues of the multidrug resistance-associated protein gene (MRP1), in human cancer cell lines. *Cancer Res* **57:**3537–3547.
Kool M, van der Linden M, de Haas M, Scheffer GL, de Vree JM, Smith AJ, Jansen G, Peters GJ, Ponne N, Scheper RJ, et al. (1999) MRP3, an organic anion transporter able to transport anti-cancer drugs. *Proc Natl Acad Sci USA* **96:**6914–6919.
Loo TW and Clarke DM (1999) Merck Frosst Award Lecture 1998. Molecular dissection of the human multidrug resistance P-glycoprotein. *Biochem Cell Biol* **77:**11–23.
Madon J, Eckhardt U, Gerloff T, Stieger B and Meier PJ (1997) Functional expression of the rat liver canalicular isoform of the multidrug resistance-associated protein. *FEBS Lett* **406:**75–78.
Merickel A, Kaback HR and Edwards RH (1997) Charged residues in transmembrane domains II and XI of a vesicular monoamine transporter form a charge pair that promotes high affinity substrate recognition. *J Biol Chem* **272:**5403–5408.
Müller M, Meijer C, Zaman GJ, Borst P, Scheper RJ, Mulder NH, de Vries EG and Jansen PL (1994) Overexpression of the gene encoding the multidrug resistance-associated protein results in increased ATP-dependent glutathione S-conjugate transport. *Proc Natl Acad Sci USA* **91:**13033–13037.
Paulusma CC, Bosma PJ, Zaman GJ, Bakker CT, Otter M, Scheffer GL, Scheper RJ, Borst P and Oude Elferink RP (1996) Congenital jaundice in rats with a mutation in a multidrug resistance-associated protein gene. *Science (Wash DC)* **271:**1126–1128.
Paulusma CC, Kool M, Bosma PJ, Scheffer GL, ter Borg F, Scheper RJ, Tytgat GN, Borst P, Baas F and Oude Elferink RP (1997) A mutation in the human canalicular multispecific organic anion transporter gene causes the Dubin-Johnson syndrome. *Hepatology* **25:**1539–1542.
Sheppard DN and Welsh MJ (1999) Structure and function of the CFTR chloride channel. *Physiol Rev* **79:**S23–S45.
Stride BD, Cole SP and Deeley RG (1999) Localization of a substrate specificity domain in the multidrug resistance protein. *J Biol Chem* **274:**22877–22883.
Stride BD, Valdimarsson G, Gerlach JH, Wilson GM, Cole SP and Deeley RG (1996) Structure and expression of the messenger RNA encoding the murine multidrug resistance protein, an ATP-binding cassette transporter. *Mol Pharmacol* **49:**962–971.
Suzuki H and Sugiyama Y (1998) Excretion of GSSG and glutathione conjugates mediated by MRP1 and cMOAT/MRP2. *Semin Liver Dis* **18:**359–376.
Taniguchi K, Wada M, Kohno K, Nakamura T, Kawabe T, Kawakami M, Kagotani K, Okumura K, Akiyama S and Kuwano M (1996) A human canalicular multispecific organic anion transporter (cMOAT) gene is overexpressed in cisplatin-resistant human cancer cell lines with decreased drug accumulation. *Cancer Res* **56:**4124–4129.
Toh S, Wada M, Uchiumi T, Inokuchi A, Makino Y, Horie Y, Adachi Y, Sakisaka S and Kuwano M (1999) Genomic structure of the canalicular multispecific organic anion- transporter gene (MRP2/cMOAT) and mutations in the ATP-binding-cassette region in Dubin-Johnson syndrome. *Am J Hum Genet* **64:**739–746.
Tsujii H, Konig J, Rost D, Stockel B, Leuschner U and Keppler D (1999) Exon-intron organization of the human multidrug-resistance protein 2 (MRP2) gene mutated in Dubin-Johnson syndrome. *Gastroenterology* **117:**653–660.
Uchiumi T, Hinoshita E, Haga S, Nakamura T, Tanaka T, Toh S, Furukawa M, Kawabe T, Wada M, Kagotani K, et al. (1998) Isolation of a novel human canalicular multispecific organic anion transporter, cMOAT2/MRP3, and its expression in cisplatin-resistant cancer cells with decreased ATP-dependent drug transport. *Biochem Biophys Res Commun* **252:**103–110.
van Aubel RA, van Kuijck MA, Koenderink JB, Deen PM, van Os CH and Russel FG (1998) Adenosine triphosphate-dependent transport of anionic conjugates by the rabbit multidrug resistance-associated protein Mrp2 expressed in insect cells. *Mol Pharmacol* **53:**1062–1067.

Send reprint requests to: Hiroshi Suzuki, Ph.D., Graduate School of Pharmaceutical Sciences, The University of Tokyo, Hongo, Bunkyo-ku, Tokyo 113-0033, Japan. E-mail: seizai.suzuki@nifty.ne.jp